

Measurement of Approach Noise Footprints of a C-17 STOL Aircraft during Conventional and Noise-Mitigating Approach Trajectories

W. Clifton Horne*, Cahit Kitaplioglu**
NASA Ames Research Center
Moffett Field, CA

Nathan J. Burnside‡
Aerospace Computing, Inc.
Moffett Field, CA

David Schein§
Northrop-Grumman Corp.
El Segundo, CA

Abigail Liddle† and Andrew Welborn†
California Polytechnic State University
San Luis Obispo, CA

Several conventional and noise-mitigating landing approach patterns were recently successfully demonstrated with a C-17 STOL aircraft, as part of an ongoing study of the integration of ESTOL-class aircraft into the national airspace system. During the demonstration, ground measurements of approach noise were obtained with an array of ground measurement stations at the NASA Dryden Research Flight Center. The measurements confirm projected trends of reduced noise impact to the greater airport vicinity for noise-mitigating approaches relative to a conventional 3° glide-slope approach.

I. Introduction

Recent improvements in air traffic routing technology, such as the Global Positioning Satellite (GPS) system and Area Navigation (RNAV), provide greater flexibility in terminal-area procedures to safely meet persistent challenges such as growing capacity and increasingly stringent noise restrictions. One example of a new procedure with demonstrated noise benefit is the Continuous Descent Approach (CDA)^{1,2,3}.

The routing flexibility enabled by these new technologies also make possible the introduction of new classes of aircraft designed to accommodate demands for increased capacity by accessing under-utilized runways at existing facilities without impacting conventional operations. Shorter, low-use runways can be accessed by civilian rotorcraft or by ESTOL (Extremely Short Take-Off/Landing) class aircraft, which utilize advanced lift-augmentation methods to reduce take-off or landing field length⁴.

Quiet STOL operations have been demonstrated by experimental aircraft such as the Quiet Short-haul Research Aircraft (QSRA)⁴. Quiet operations can also be achieved through a combination of quiet high-lift technology on the aircraft combined with new noise-mitigating procedures facilitated by RNAV.

* Aerospace Engineer, Associate Fellow AIAA.

** Aerospace Engineer

§ Aerospace Engineer, Member AIAA

‡ Aerospace Engineer, Member AIAA

† Student Member AIAA

A demonstration of potential noise-mitigating approach procedures was recently conducted in a cooperative study between NASA's Ames Research Center and Dryden Flight Research Center using a C-17 STOL transport. Researchers from Northrop-Grumman and students from California Polytechnic State University-San Luis Obispo also participated in this study.

During the demonstration, three approach procedures were flown primarily to evaluate operability and ride quality. The three procedures consisted a conventional 3° straight-in approach, a steeper 5° straight-in approach, and a novel spiral descent pattern, which will be described in detail in the following section. The latter procedure, termed as Simultaneous Non-Interfering (SNI) approach permits the aircraft to enter the airspace over the airport at a relatively high altitude and descend to the final approach glide-slope within the airport boundary.

Prior to the flight demonstration, 17 noise-measuring systems were assembled and calibrated. These systems were positioned under the flight tracks to record noise levels during the demonstration procedures. A complete description of these systems is given by in a separate report, but will be briefly described in the following section.

Selected flight parameters were recorded by the aircraft flight data system and coordinated with the ground-based noise-measuring systems. The time histories of position, airspeed, and thrust were input to a noise simulation of the C-17 using Integrated Noise Model (INM), which will be compared with the measured noise records.

2. Test set-up

Test aircraft and runway

The test aircraft was a Boeing C-17, equipped with four F117-PW-100 turbofan engines. The aircraft was equipped with a flight data recorder that logged aircraft position, airspeed, attitude, and control settings approximately 12 times/sec. Prior to the flight demonstration, the three approach procedures were evaluated on the NASA DFRC C-17 flight simulator and programmed into the aircraft's autopilot system. However, the autopilot was not configured for high wind speeds and the procedures were flown manually on the day of test.

The C-17 is capable of operating in conventional high-lift approach configuration, as well as powered-lift mode for shortest landing roll. In the latter mode, the flaps are extended to deflect the engine exhaust downward for enhanced lift and slower landing speed. During this demonstration, the aircraft was operated only in the conventional-lift configuration, with landing gear deployed. The pilot was also instructed to maintain as constant a thrust level as possible during the demonstration to minimize variation in noise due to changing thrust.

The primary objectives of the demonstration were in-flight evaluations of operability and ride quality. The aircrew and a commercial aircraft pilot-observer provided assessments. Results of these evaluations will be conveyed in a separate report. The secondary objective was to obtain comparative measurements of approach noise to document differences in ground noise between the profiles.

To conserve operating time and fuel, the demonstration program consisted of 12 approach descents to within about 200 ft of the surface, followed by a full-thrust pull-out and return to pattern for the next approach. The demonstration was conducted on a Saturday morning at Runway 17C to minimize noise interference from routine base operations.

Approach trajectories

The standard 3° straight-in approach is shown in Fig. 1a. For FAR Part 36 certification, noise on approach is measured 2000 m (6562 ft) from the threshold. With a 3° glide-slope, the aircraft passes 120 m (394 ft) over this location and 15 m (49 ft) over the threshold. Fig. 1b shows the steeper 5° straight in approach, with altitudes of 190 m (623 ft) and 15m (49 ft) over the certification and threshold locations, respectively.

3° approach: ref: NASA RP-1258 v2

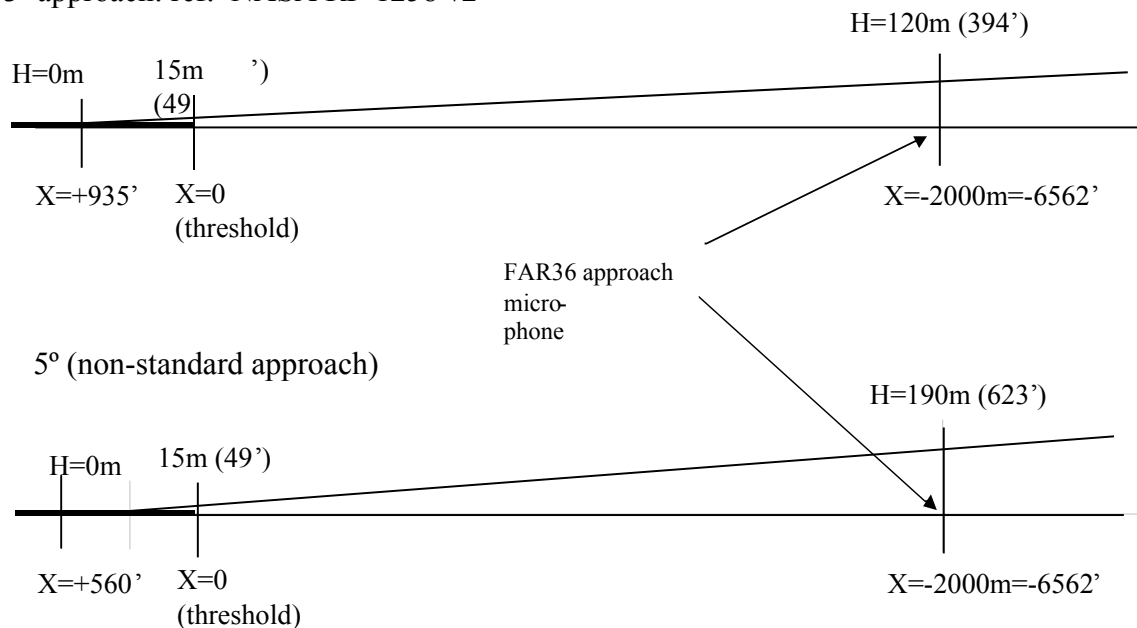


Fig 1a,b. Profiles of 3° and 5° glide slope straight-in approaches.

The model SNI spiral-descent procedure selected for this demonstration is shown in fig. 2. It consists of a 0.71 nm (2621 m, 4300 ft) radius circular track tangent to the 2000m approach certification location. The aircraft enters the circular track at about 2650 ft AGL, and exits the circle at about 600 ft AGL. The radius was selected following C-17 simulation runs to limit bank angle and G-loading to levels typical in current commercial flight procedures.

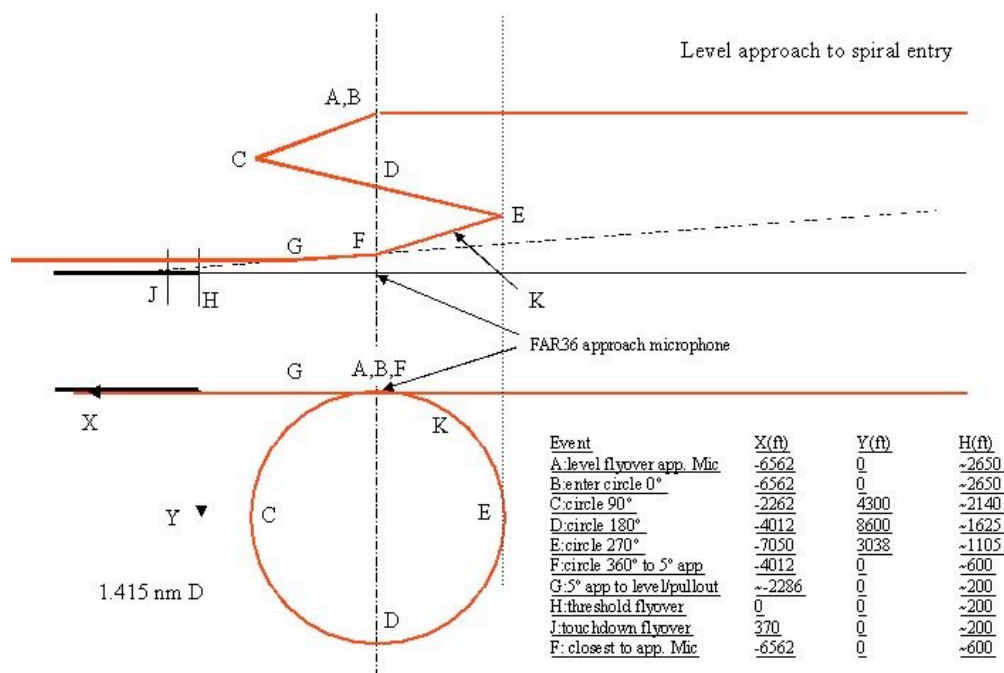


Fig. 2. Model spiral SNI descent from level approach.

The steeper 5° approach reduces noise under the flight track both by allowing a lower engine power setting and larger distance from the aircraft noise source to the ground.

Neglecting differences in airspeed and engine power setting, both the spiral-descent SNI and 5° straight-in approaches should be quieter over the runway CL during the initial approach than the 3° conventional approach due to the higher altitudes, as shown in fig. 3. The SNI approach introduces an increased noise area under the circular track segment, but this will be within the boundary of most civilian airports.

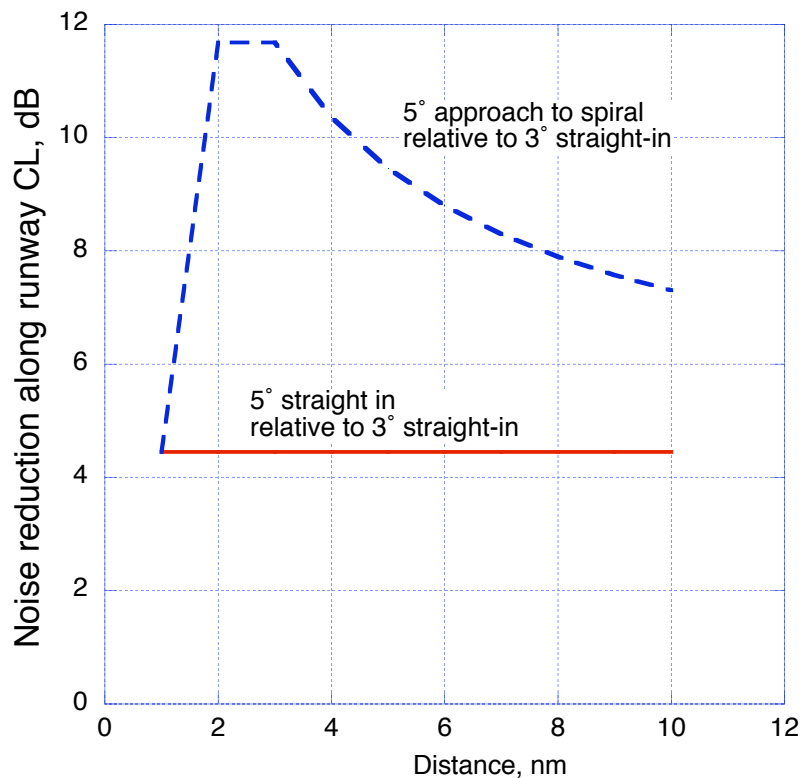


Fig. 3. Noise reduction of 5° straight in and spiral SNI descent (from 5° initial entry) relative to conventional 3° descent. Projected reduction is only for the linear track segment (excludes spiral segment).

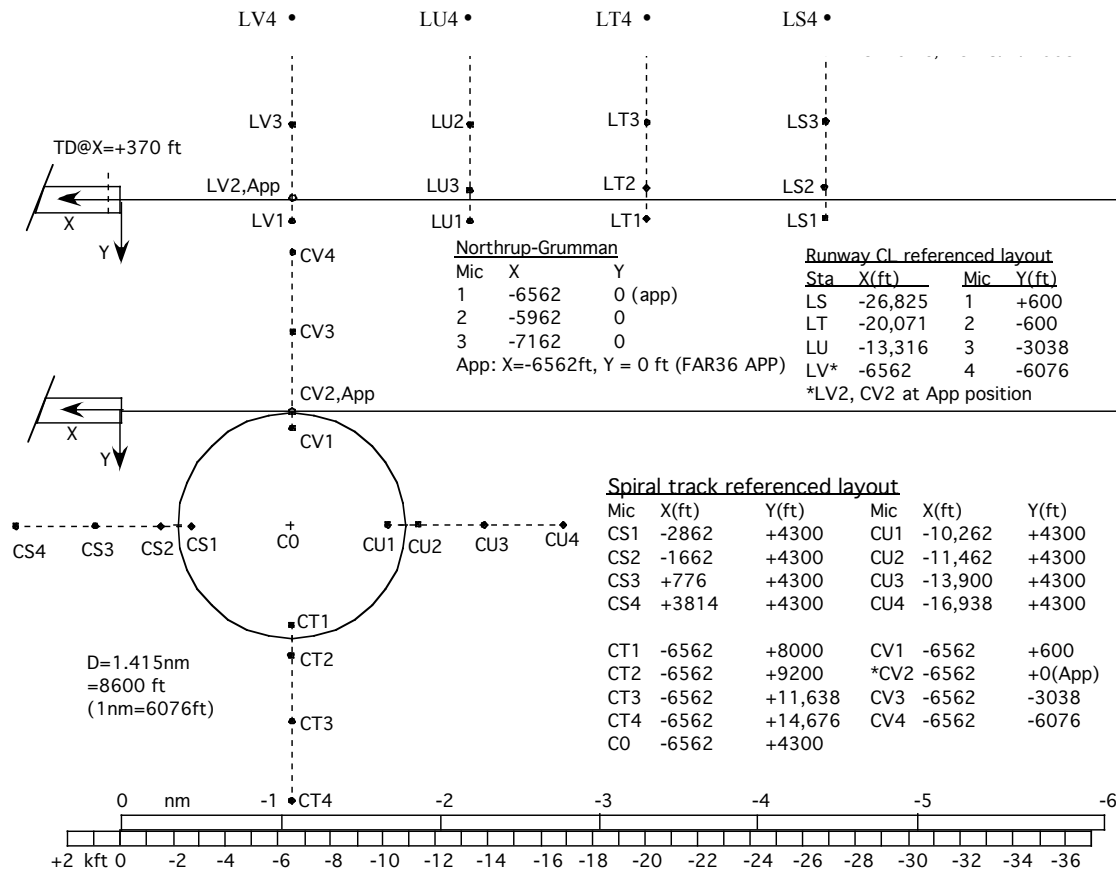


Fig. 4. Ground microphone measurement locations for the rectangular (L) and circular (C) patterns. Note that the V1-V4 locations are identical for both patterns.

Ground microphone locations.

Several constraints guided the selection of microphone locations. The microphone ground stations needed to be located within the boundary of the approximately 8-mi. diameter Rodgers Dry Lake, away from surrounding highway traffic and ground operations. The desired spatial coverage exceeded available cable lengths, and RFI concerns ruled out the use of wireless control, so 17 independent PC-laptop based systems were configured for this test. To assure adequate coverage of the different approach patterns, two location patterns were selected, as shown in fig. 4. The “C” (circular) pattern consisted of four microphones on each of four lines radiating from the center of the spiral descent approach pattern, extending up to 1 nm outward from the aircraft ground track. A single microphone was placed in the center of the circular track.

The second, or “L” pattern (linear) was rectangular with the same ground-track displacements from the threshold as the four radial stations of the circular pattern. This allowed for direct comparisons of the effects of curved-track approaches versus conventional straight-in approaches on the noise footprints. The circle-center microphone was also used for the rectangular pattern.

For both patterns, the four ground-track stations were labeled S,T,U, and V in order of approach. Note that the V-line of microphones was common to both patterns and positioned at the approach certification displacement (2000m or 6562 ft). At each station, microphones were located 600 ft. right, 600 ft. 0.5 nm and 1.0 nm left of ground track. Northrup-Grumman Corp. also provided three ground-plane microphones on the V-line (approach certification locations LV2 and CV2) on and 600 ft to the left and right of the ground track.

Ground microphone measurement systems

Each microphone location was supplied with a self-contained sensor, signal conditioning, and data acquisition system. A detailed discussion of the development and characteristics of the measurement system and data processing methods will be reported separately. A block diagram of the system is given in fig. 5. Each system used a B&K 4133 microphone, a TMS type 126AC preamplifier, and a TMS type 112A battery-powered power supply. The microphones were flush-mounted in a 24" sq. plywood plate supported 4" above the ground. The ground surface was flat, hard, dry lakebed. The microphone signal was digitized by a Creative Labs SoundBlaster 24-bit PCMCIA sound card installed in PC-laptop computers provided by ODIN IT services at Ames, running a custom LABVIEW acquisition script. Prior to the test, the frequency response function of each sound card, digitizing at 22.05 kHz, was measured and applied as a correction in the processing software. Location and time synchronization information was provided by GPS modules installed in each measuring system computer.

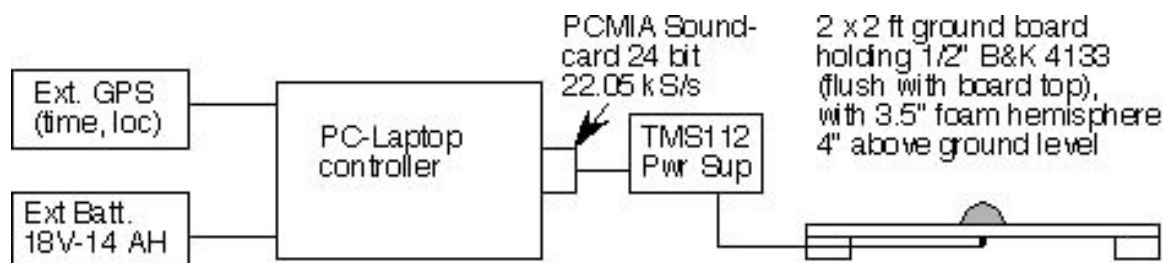


Fig. 5. Block diagram of typical ground microphone station, 1 of 17.

After deployment, each measurement station was powered up and stabilized for at least 20 min. Each microphone was then calibrated with a B&K pistonphone at a level of 124 dB, corrected for the local altitude of 2300 ft. Data measurements were acquired as 240 second continuous records initiated verbally over radio. At the end of the test, all records were uploaded to a single processing computer. The time records were transformed to 1024 pt FFT's, with Hanning window and no overlap. Successive FFT's were averaged over 1/2 second intervals, and further processed to generate 1/3-octave and A-wt levels from 50 to 8000 Hz. Additional overall metrics such as maximum A-weight level, SEL, EPNL, etc were then derived from the 1/2 second interval records for each microphone using standard definitions. The discussion in this report is focused on maximum A-weight level, denoted as L_{AMAX} .

Weather and environment

Wind speed, direction, temperature, and humidity were recorded at the approach certification location at 3-minute intervals during the flight demonstration. The wind was consistently from the SW from 12 to 29 knots. This level exceeded allowable winds for certification, and resulted in background noise levels from 50-60 dBA. For most of the runs however, the peak noise from the aircraft along the ground track was at least 10 dB above background noise, therefore these data will be the primary topic of discussion in the following section. Temperature and relative humidity conditions were within certification limits for all measurements.

The time schedule of the test was dictated by availability of resources and staff, and could accommodate weather delays only in the event of precipitation or visibility impacting the primary objective of assessing operability and ride quality.

A table of the test measurements taken on 9/10/05 is given below in Table 1:

Run	Start	Duration	Pattern	Trajectory	Temp, °F	RH%	Wind-kt	Comment
100A	08:03	20 sec	circ	N/A	64	59	16 SW	Bckgrnd. noise
113	08:13	240	circ	5° straight	65	57	14 SW	
110	08:52	240	circ	SNI spiral	68	48	17 SW	
111	09:08	240	circ	SNI spiral	69	46	23 SW	
112	09:20	240	circ	SNI spiral	70	44	20 SW	
100B	10:50	20	rect	N/A	74	31	18 SW	Bckgrnd. noise
102	11:34	240	rect	3° straight	76	28	29 SW	
103	11:45	240	rect	3° straight	77	27	22 SW	
104	12:06	240	rect	5° straight	78	27	27 SW	
105	12:20	240	rect	5° straight	79	26	23 SW	
106	12:33	240	rect	5° straight	79	25	24 SW	
107	12:45	240	rect	SNI spiral	78	24	26 SW	
108	12:57	240	rect	SNI spiral	80	23	26 SW	

Table 1: Test run conditions

3. Test results

Ground tracks and flight profiles

Information from the flight data recorder provided invaluable information for both the primary objective of assessing operability and the secondary objective of documenting the ground noise characteristics of each procedure.

The coordinate system for this report has X positive in the flight direction, Y positive from the pilot to the left wing tip, and Z positive upwards, with the origin at the runway threshold centerline. Fig. 6 shows an overhead view (XY) of the two spiral SNI descents (runs 107,108) over the rectangular microphone pattern, with microphones represented as 'x' symbols. The circular pattern field microphone locations are shown for clarity as 'o' symbols. Although not shown, the overhead views of the 3° (runs 102,103) and 5° (runs 104,105) straight in descents line up almost exactly with the straight portion of run 108. Note that the approach progress from left to right. Ideally the flight track would fall midway between the two closest microphones at each station. For almost all of the procedures, the aircraft passed directly over the left-most microphones of the rectangular pattern and the second innermost microphones of the circular pattern. Signals from the microphones closest to the respective ground tracks will be discussed in detail in the following section.

Vertical profiles (XZ) of the three descents over the rectangular pattern are shown in fig. 7. Note that the horizontal scale factor is approximately 9 times the vertical factor. During the 3° descent, the airspeed was maintained at a nearly constant 145 kts, and at 120 kts for the 5° and spiral SNI descents. For the 3°, 5° and spiral SNI descents, the EPR was maintained at approximate values of 1.1, 1.07, and 1.06 respectively. Also note the slightly higher descent rate for the spiral SNI descent relative to the 5° straight-in descent, reflecting the pilot instructions to maintain engine speed rather than descent rate. During the spiral SNI descent the roll attitude was approximately 10 deg left wing down.

Overhead views (XY) of the spiral SNI descents over the circular microphone pattern are shown in fig. 8. Except for run 110, (which was the first flight of the spiral descent), the ground tracks for run 111 and 112 are similar to the spiral descent tracks discussed previously. Corresponding vertical profiles (XZ) of the 3 spiral SNI descents (runs 111-113) and the single 5° straight in approach are shown in fig. 9. Airspeeds and engine settings for these runs are similar to those discussed previously.

In terms of operability and ride quality, the pilot was able to accurately hold and repeat the scheduled approaches and the commercial pilot evaluator rated the procedures as benign, in spite of the lack of autopilot control and the strong headwinds.

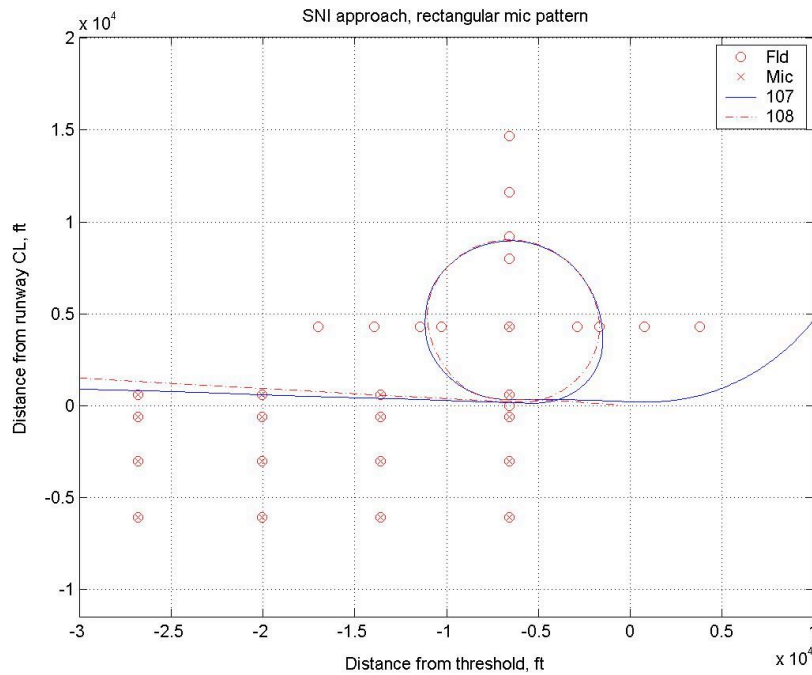


Fig. 6. Overhead view (XY) of spiral SNI approaches 107 and 108 over rectangular microphone pattern. 3° and 5° approaches were very close to the linear segment of run 108.

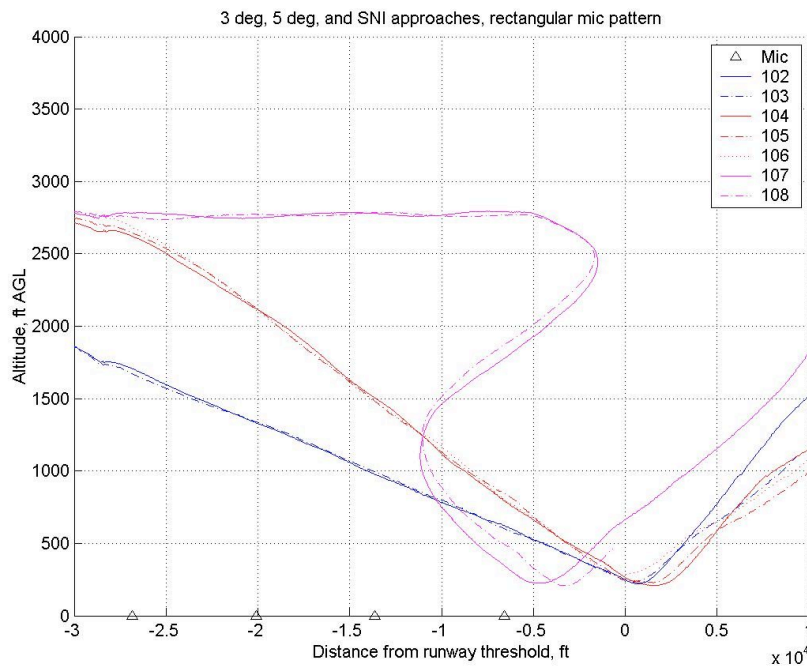


Fig. 7. Vertical profile (XZ) for 3° straight-in approaches 102, 103; 5° straight-in approaches (runs 104-106); and spiral SNI approaches (runs 107-108) over rectangular microphone pattern. Note that vertical scale is 9x resolution of horizontal. Power setting for all approaches was nearly constant.

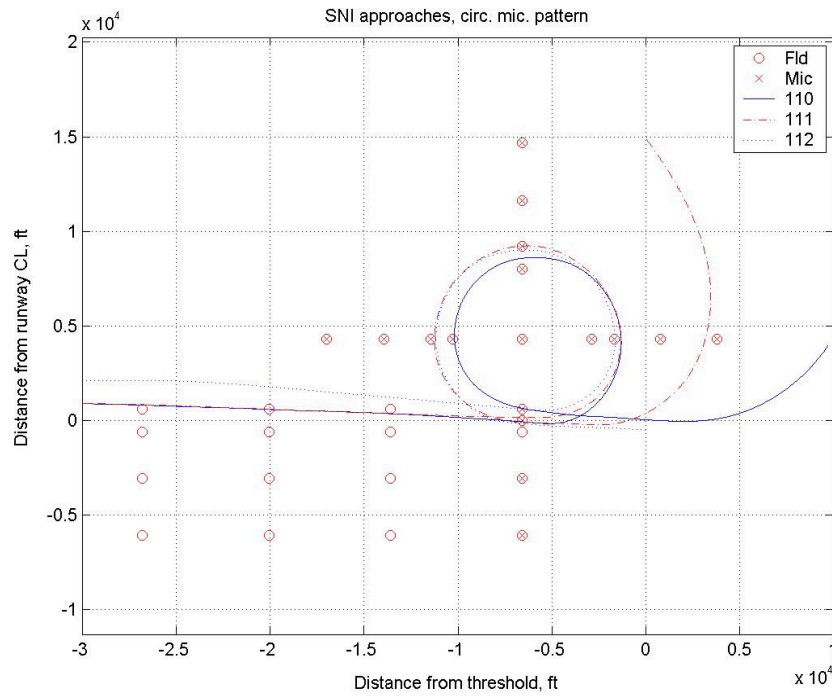


Fig. 8. Overhead view (XY) of spiral SNI approaches 110, 111, and 112 over circular microphone pattern.

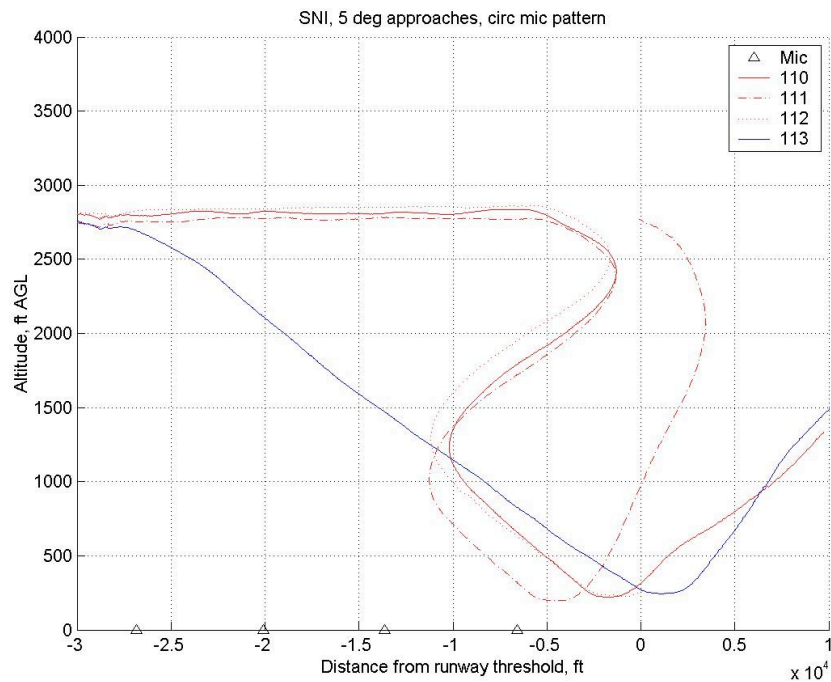


Fig. 9. Vertical profile (XZ) of 5° straight-in approach 113 and spiral SNI approaches 111-113 over circular microphone pattern. Horizontal scale is $\sim 9\times$ vertical scale.

Discussion of noise measurements

Fig. 10 shows A-weighted levels (0.5 second averaging interval) for the four microphones directly under the ground track of the 3° straight-in descent over the rectangular microphone pattern, run 102. The base noise level (wind and aircraft noise) varies from 55 to 62 dBA, while the peak flyover noise levels vary from 72 to 85 dBA, 10-23 dBA higher than the base level. In general, the peaks are well defined and relatively free of random variations. The time scale is in seconds relative to an arbitrary start time.

Fig. 11 shows corresponding levels for four microphones directly under the ground track of the 5° straight-in descent over the rectangular microphone pattern, run 106. As expected the levels for the first two microphones (LS1, LT1) are lower (approximately 70 dBA peak) than for the 3° descent due to the higher approach altitude, while the last microphone shows a level (LV1) comparable to the value for the 3° descent. Rapid variations in level are more apparent at the lower flyover noise levels.

Fig. 12 shows levels for the four microphones directly under the ground track of the spiral SNI approach over the rectangular microphone pattern, run 108. The initial constant-altitude flight over the four microphones closest to runway centerline results in nearly constant peak levels for those events. A large peak of 85 dB is registered over LV1 when as the airplane exits the spiral for final descent. Since LV1 is closest to the approach certification location, it can be seen that an approach certification level for this procedure is not indicative of levels farther from the threshold.

Fig. 13 shows levels for the four microphones directly under the ground track of the spiral SNI approach over the circular microphone pattern, run 112. The aircraft is steadily descending as it proceeds over CS2, CT2, CU2, and CV1, which accounts for the steadily increasing peak levels as it continues through the spiral descent segment.

Relative trends in noise over the initial linear segments of the three procedures are shown in fig. 14, for the 3° straight-in (102,103), 5° straight-in (104-106), and spiral SNI (107,108) approaches over the four microphones directly under the ground track of the rectangular microphone pattern. Plotted are local peak A-weight levels, 0.5 second averaging time. As predicted (in fig. 3), the spiral SNI approach maintains the lowest noise level, a nearly constant 72 dBA over the linear segment. The 5° and spiral SNI approaches begin with comparable levels over LS1, and then increase as they approach the threshold. Over LV1, the 5° and 3° approaches are louder than the initial spiral-SNI event by about 5 and 10 dBA respectively, close to projected values.

It is also useful to compare relative values of peak A-weight levels between the 5° descent over the rectangular pattern microphones (see fig. 14) with the circular pattern microphones under the path of the spiral SNI descent, as shown in fig. 15, since the patterns were designed to yield similar ground track distances between microphones. For comparison, the spiral SNI descent peak levels have been scaled to the consistently higher altitudes of the 5° straight-in approach over corresponding ground track microphones. As discussed previously, the higher descent rate of the aircraft in the spiral SNI procedure resulted from pilot instructions to maintain constant approach thrust for the three different approaches. The trends are roughly similar, with considerable scatter.

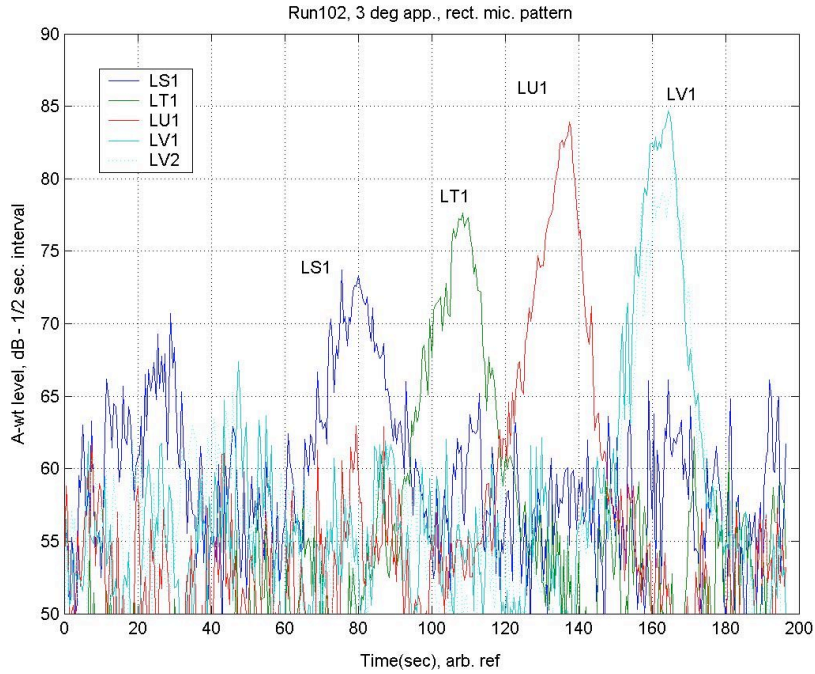


Fig. 10. Time histories for A-weight levels of microphones under flight track of the C-17 in 3° straight in approach, rectangular microphone pattern, run 102. Arbitrary start time, 1/2 second averaging interval.

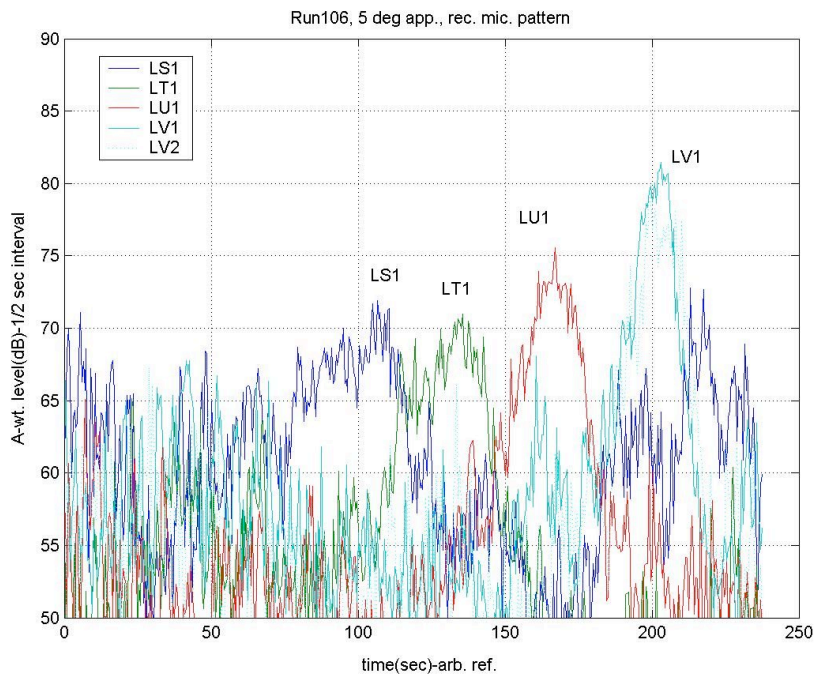


Fig. 11. Time histories for A-weight levels of microphones under flight track of the C-17 in 5° straight in approach, rectangular microphone pattern run, 106.

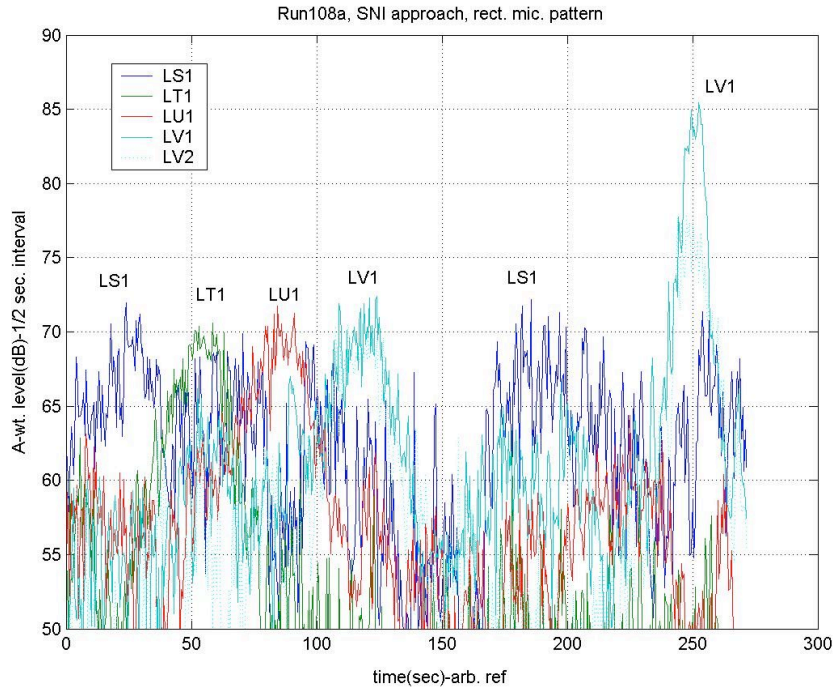


Fig. 12. Time histories for A-weight levels of microphones under flight track of the C-17 in spiral SNI approach over rectangular microphone pattern, run 108.

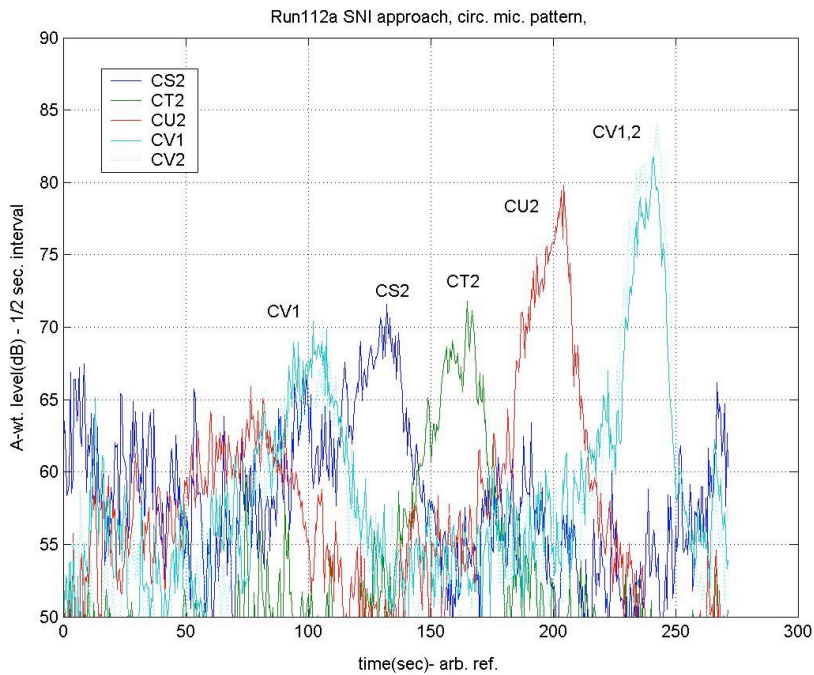


Fig. 13. Time histories for A-weight levels of microphones under flight track of the C-17 in spiral SNI approach over circular microphone pattern, run 112. Levels as recorded (unscaled for altitude).

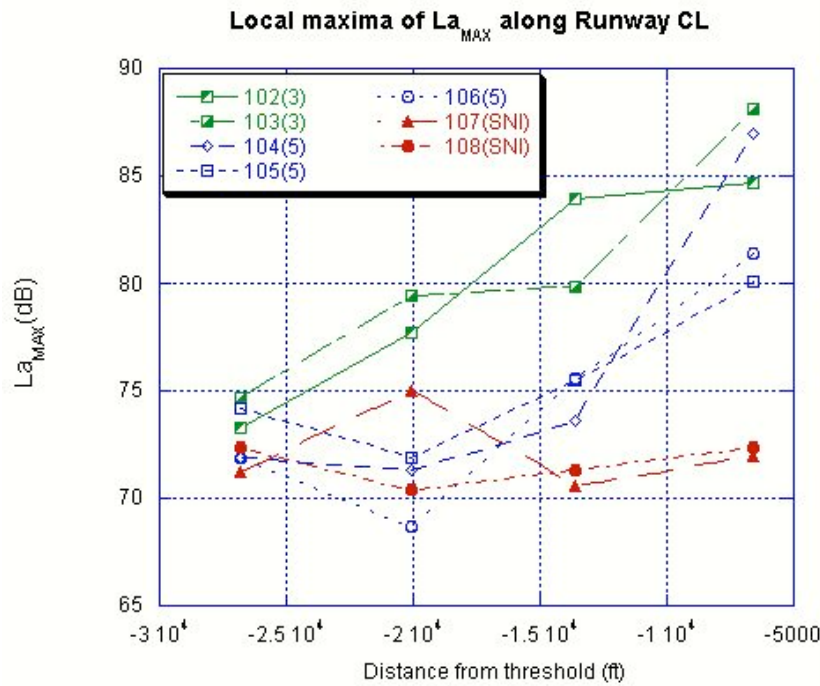


Fig. 14. Comparison of peak A-weight levels of ground track, rectangular pattern microphones under 3° straight-in (102,103), 5° straight-in (104-106), and spiral SNI (107,108) C-17 approaches. 1/2 second averaging time.

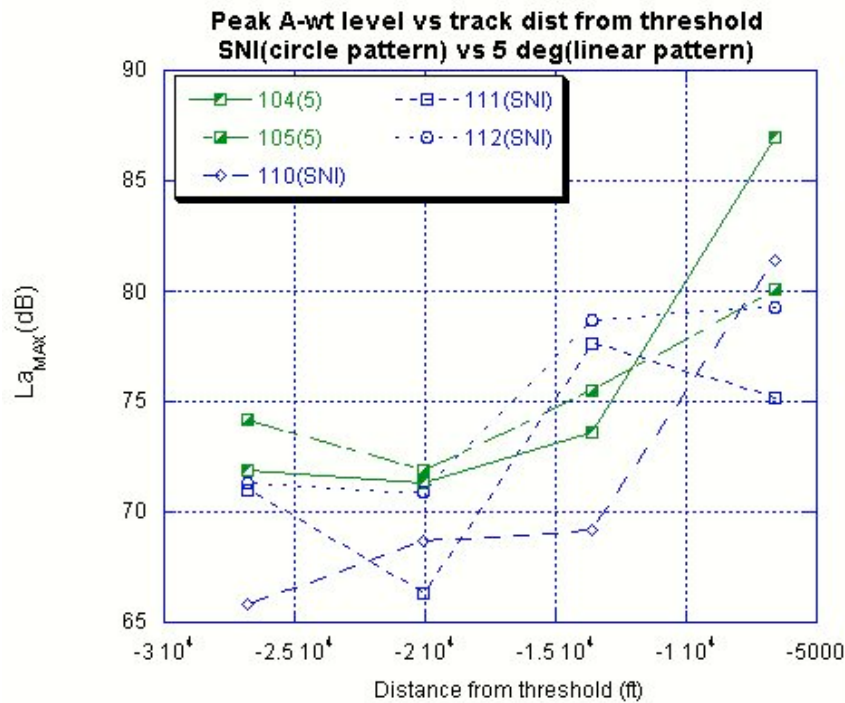


Fig. 15. Comparison of peak A-weight levels of ground track microphones for the C-17 in 5° straight-in approach over rectangular microphone pattern, vs. spiral SNI approach over circular pattern microphones. The spiral SNI circular pattern microphone levels have been scaled to the same altitude as comparable 5° straight-in approach rectangular pattern altitudes.

Lateral and radial variations in noise level

Thus far, only levels from microphones under the flight track have been discussed. Also of interest are levels at locations displaced laterally from linear track segments or radially from circular arc track segments. Levels at locations displaced from the ground track are less than ground track levels for noise sources which are non-directional in the plane normal to the flight path. For this test, the high background noise levels associated with high wind noise over microphones that were farthest from the ground track. However, lateral/radial roll-off in levels was observed in the closer microphones.

Fig. 16 shows a contour plot of peak A-weight levels for the 3° straight-in approach run 102 over the rectangular pattern. Interpolated levels between microphones are linear with pressure squared. The levels have been corrected for atmospheric attenuation and scaled for distance to an average flight path for the two 3° approaches. Note that for fig. 16, 17, and 18, the horizontal and vertical scales differ by a factor of about 9.

Fig. 17 shows a similar contour plot for the 5° straight-in approach run 106 over the rectangular pattern. The trend of lower noise levels for this steeper approach is clearly apparent. The background noise floor is measured at the two furthest locations from the ground track.

Fig. 18 shows the contour plot for the spiral SNI approach run 108 over the rectangular pattern. The higher noise level associated with the exit of the spiral procedure is seen at the approach microphone LV1.

Fig. 19 shows the contour plot for the spiral SNI approach run 112 over the circular pattern. As in the previous figure, the highest noise level is observed over the LV1/CV1 microphone when the aircraft is at minimum altitude.

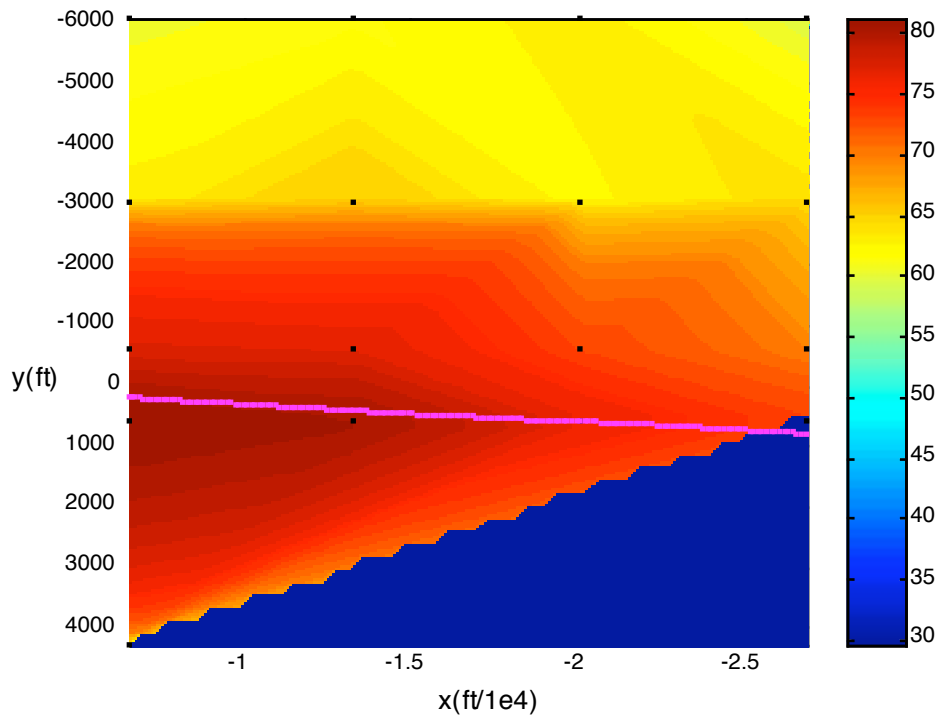


Fig. 16. Contours of peak A-weight level for 3° straight in approach over rectangular microphone pattern, run 102.

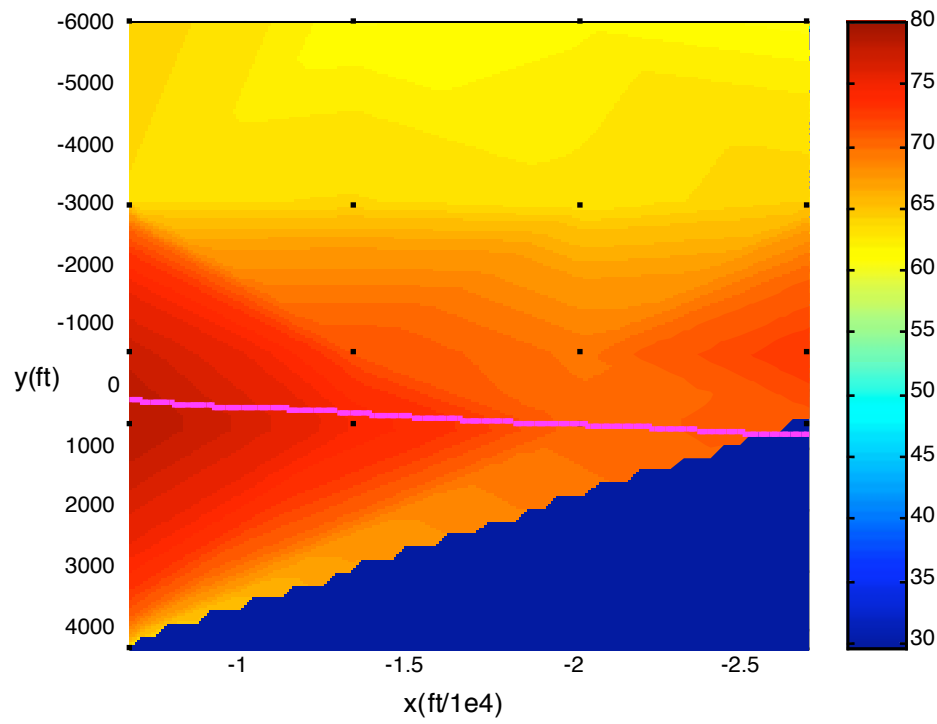


Fig. 17. Contour map of peak A-weight level for the 5° straight-in approach run 106 over the rectangular microphone pattern, run 106.

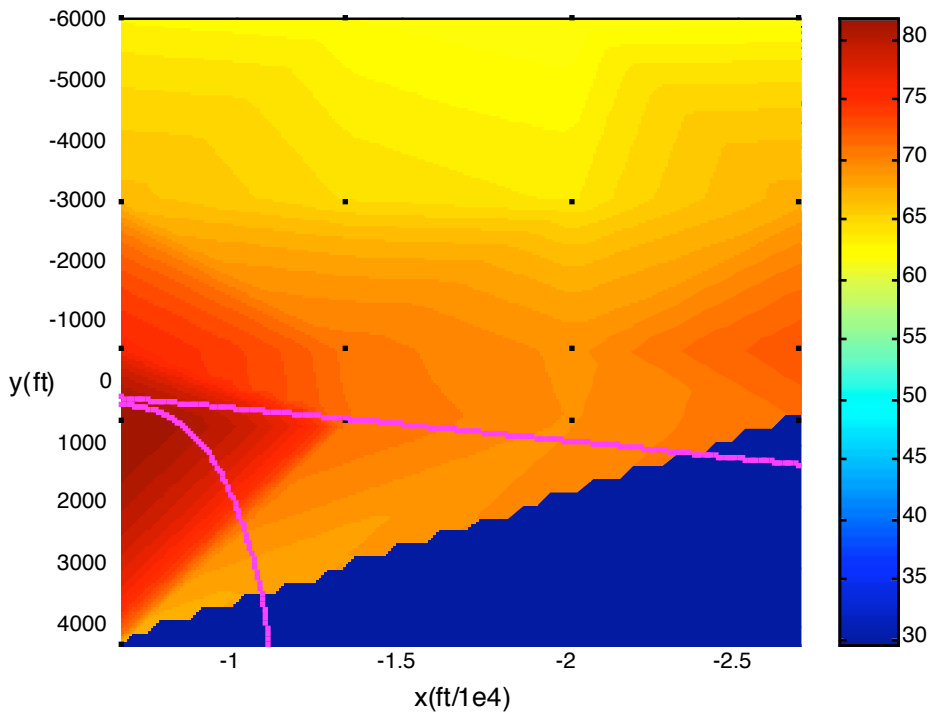


Fig. 18. Contour plot of peak A-weight level for spiral SNI approach over rectangular pattern, run 108.

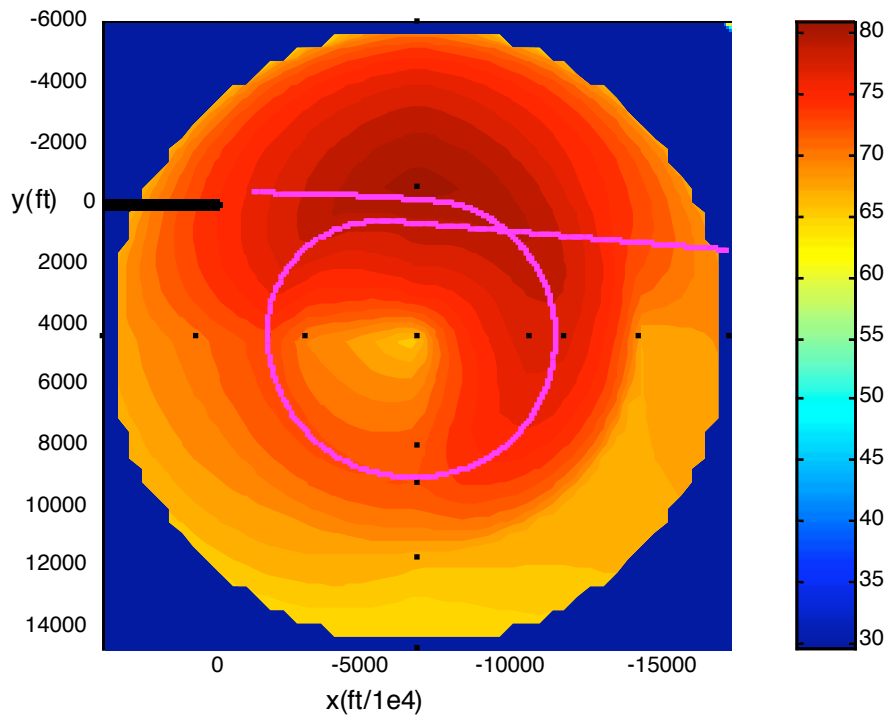


Fig. 19. Contour plot of peak A-weight level for spiral SNI approach over circular pattern, run 112.

4. Comparison with predictions

Several airport noise prediction tools, such as the FAA's Integrated Noise Model (INM), are available and are in routine use for land use planning and environmental review. These tools are appropriate for typical airport operations, and are not intended for comparison with measurements of single events. However, it is anticipated that research programs similar to the present study can contribute to verify the trends predicted by these tools, and to the eventual incorporation of ESTOL and other non-conventional aircraft in the prediction tool databases.

INM includes predictions of noise from civilian and military aircraft in standard approach, take-off, and fly-over procedures, as well as algorithms for predicting noise from civilian (but not military) aircraft in user-defined procedures. For this study, the flight data records of position, airspeed, and engine RPM were processed using Mathwork's MATLAB and Microsoft's EXCEL programs into INM-compatible files to enable comparisons of overall noise-contour shape and peak levels of maximum A-weighted level. For each predictions the flight data record was re-sampled during the aircraft's passage over the area enclosing the linear and circular microphone patterns to conform to INM's limit of 999 position points. Predictions of maximum A-weight level (LMAX) for flight data from the four approaches (runs 102, 106, 108, and 112) are presented in figures 20, 21, 22, and 23 respectively. Note that each plot exhibits the artifact of abrupt beginning and ending of the flight data record.

In each case the inner-most contour is 85 dB LAMAX, and the green and yellow areas are separated by the 65 dB contour. Each plot has been rotated so that the runway 17C centerline is horizontal. The tick marks are 1 nm intervals in the true N-S direction. The lines of microphones closest to the runway threshold (LV, CV) were 1.08 nm (6562 ft, 2000m) from the threshold, the line of microphones in the rectangular array farthest from the threshold were 2.79 nm (16,938 ft, 5163 m). In these figures, the horizontal and vertical scales are equal

Direct comparisons between INM predictions and the measurements are difficult with the sparse measurement grid, however it is useful to compare levels at a few locations along the ground track.

The following table compares levels at the closest (LV: 1.08 nm from threshold) and farthest (LS: 2.79 nm from threshold). The levels generally agree to within 2-3 dB, except for the case of run 108 2.79 nm from the threshold.

Run	1.08 nm meas.	1.08 nm INM	2.79 nm meas	2.79 nm INM
102 (3° straight-in)	80 dB LAMAX	80	72	75
106 (5° straight-in)	80	78	72	70
108 (SNI spiral)	82	80	72	62
112 (SNI spiral)	81	82	N/A	N/A

Table 2: Comparison of measured and predicted (INM) levels of LAMAX along ground track 1.08 and 2.79 nm from threshold

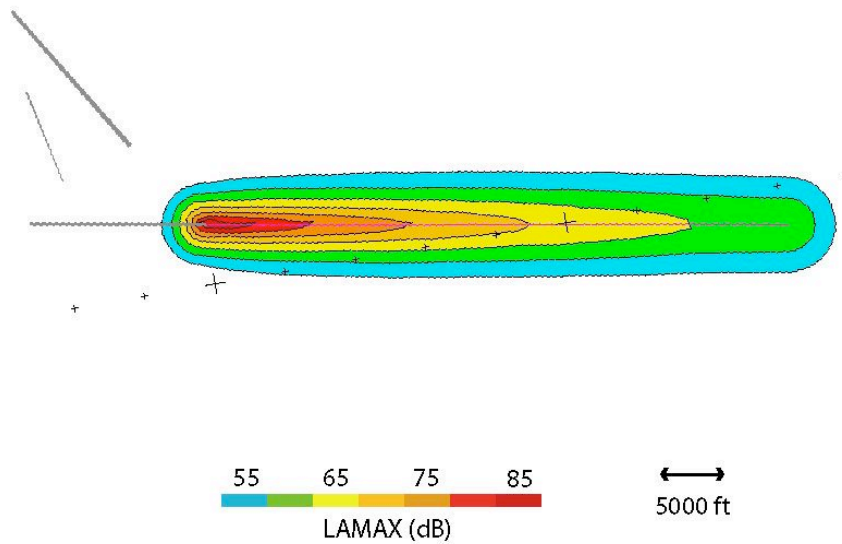


Fig. 20. Single-event INM prediction of C-17 for 3° straight-in approach, run 102.

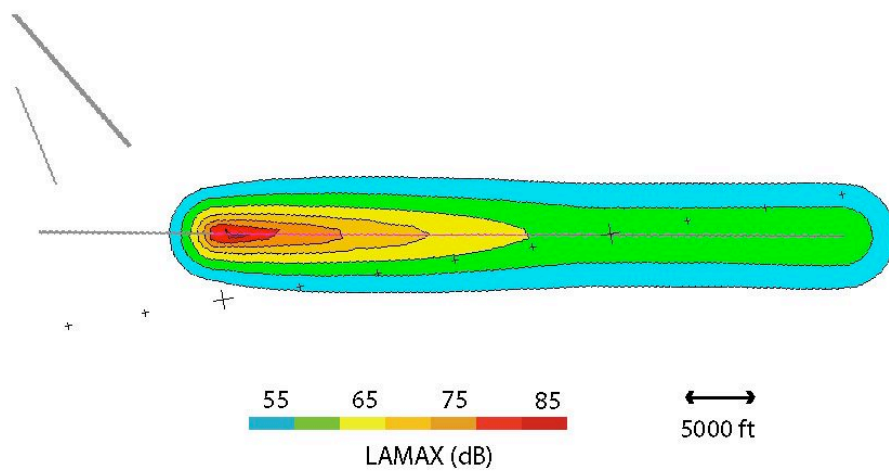


Fig. 21. Single-event INM prediction of C-17 for 5° straight-in approach run 106.

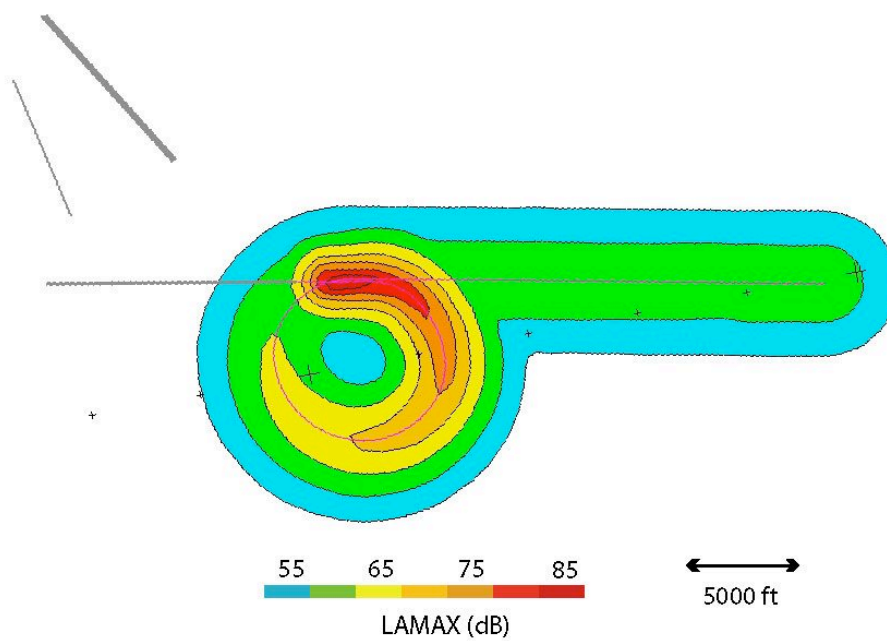


Fig. 22. Single-event INM prediction of noise for SNI spiral approach run 108.

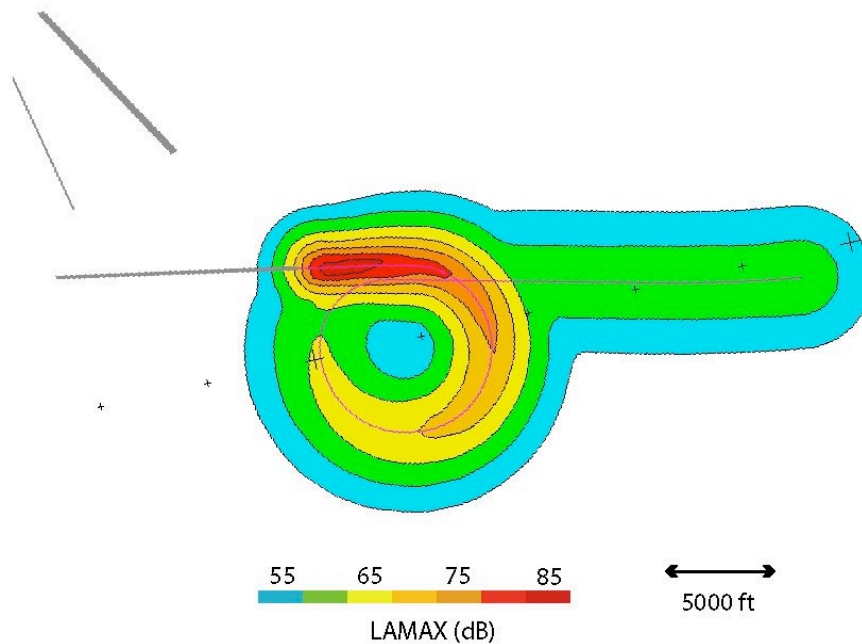


Fig. 23. Single event INM prediction for SNI spiral approach run 112.

Another interesting observation from the INM predictions is the displacement of the 65 dB LAMAX contour from the threshold along the ground track: approximately 6.8 nm for run 102 (3° straight-in), 4 nm for run 106 (5° straight in) and 1.5-2 nm for runs 108, 112 (SNI spiral). Further reductions for the SNI-spiral approach would be expected for a 5° descending entry into the spiral descent, rather than the level entry flown during this test.

5. Concluding remarks

In a recent flight demonstration of a C-17 STOL transport at NASA Dryden Flight Research Center, ESTOL-type approach procedures, including 5° straight-in and spiral SNI approaches, were compared with conventional 3° approaches to assess operability, ride quality, and effects on ground noise. The ground noise was measured with 17 independent PC-laptop based systems, each equipped with 24-bit PCMIA sound card, GPS receiver, external battery, condenser microphone sensors and power supplies. The demonstration successfully completed all objectives. High but consistent surface winds throughout the demonstration did not adversely degrade repeatability of the flight trajectory, but did result in elevated background noise levels. Signal-to-noise ratio for microphones under the flight track were sufficient to consistently determine peak noise levels. Relative differences between peak noise levels between the three approach procedures agreed well with simple estimates based on altitude.

File conversion algorithms were developed and implemented to develop predictions from FAA's Integrated Noise Model based on actual flight trajectories, airspeed, and engine settings. Measurements displaced laterally 0.5 to 1 nm from the ground track exhibited high background noise levels due to high wind conditions, however microphones near the ground track generated usable signals which generally agreed with the INM predictions.

Acknowledgements

This project was sponsored by the NASA Vehicle Systems Program, Dr. Richard Wlezian, Manager

The successful outcome of the novel flight demonstration was due to the hard work and close cooperation of a large team of engineers and flight crew from NASA Ames, NASA Dryden, US Air Force, Aerospace Computing, Ind, Centra Corp., Northrop-Grumman Corp., and professors and students from California Polytechnic Institute, San Luis Obispo. The authors express their gratitude to all.

NASA Ames: Craig Hange, Tim Naumowicz, Steve Walker, Doug Wardwell, Dave Yaste, John Zuk

NASA Dryden: Russ Barber, Marta Bohn-Meyer, Frank Batteas, Doug Coffin, Jim Farber, John Heinzman, Chris Miller, Jim Smolka, John Spooner, Mike Venti

US Air Force: Phil Dyer, Chris Elenbaum, Landon Henderson, Jonathon Henry, Kelly Latimer, Barth Shenk

Aerospace Computing: Bryan Reinero, Bruce Storms

Centra Corp. Dennis Eckenrod, Matt Peperak

Northrop-Grumman: David Graham

Cal Poly: Prof. David Hall, Prof. Mark Waters, Cassy Anthony, Joshua Caldwell, Erika Berg, Laren Fong, Erik Kurth, Brady Mitchell, Julie de la Montanya, Zachary Nichols, Scott Peery, Natalia Sanchez, Katherine Van Dellen

References

1. Gershzhom, et al, "Advanced Noise Abatement Procedures, an Experimental Study of Flight Operational Acceptability, AIAA-2002-5867.
2. Elmer, et al, "Community Noise Reduction using Continuous Descent Approach: Flight Demonstration Flight Test at Louisville", AIAA 2003-3277.
3. Becher, et al, "Techniques for Empirical Validation of Flight Modelling Parameters Used in Terminal RNAV Procedure Design', AIAA 2004-6266.
4. Zuk, et al, "Adaptive Air Transportation System – A Catalyst for Change", AIAA-2002-5956.